applied sciences

MDPI

Article

Evaluation of Liquefaction Properties of East Coast Sand of New Zealand Mixed with Varied Kaolinite Contents Using the Dynamically Induced Porewater Pressure Characteristics

Roohollah Kalatehjari * and Ademola Bolarinwa

Built Environment Engineering Department, School of Future Environments, Auckland University of Technology, Auckland 1010, New Zealand
* Correspondence: r.kalatehjari@aut.ac.nz

Featured Application: Preliminary testing and educational purposes.

Abstract: In earthquake geotechnical engineering, physical model experiments have proven to be significant and valuable in understanding the complex physics and engineering behaviors of prototype undrained soils in fields. An executed literature review indicated that large-scale physical model testing, such as shaking table (ST) and centrifuge devices, have associated advantages and limitations. The current paper presents the design, fabrication, and calibration of a 600N-capacity, small-scale, one-directional (1-D) laboratory ST device that enables quick and valuable assessment of soil liquefaction mechanisms. The dynamically induced porewater pressure (PWP) generation characteristics of sand soil mixed with different percentage weights of clay were evaluated and illustrated as a case study for testing the ST device's performance. The east coast sand (ECS) of New Zealand's North Island was mixed with different percentages of kaolinite clay to produce five variants of ECS (00, 05, 10, 20, 25, and 30). Three input sine wave ground motions of a constant frequency of 10 Hz and amplitudes of 2, 3, and 4 were applied and classified in the current study as low, intermediate, and moderate ground motions, respectively, to evaluate the evolution of the dynamic excess pore pressures in the soil samples. The results indicated that the clean ECS and mixed samples with lower clay content (ECS00, ECS05, ECS10, and ECS15) produced the highest excess PWP throughout the three shaking cycles, with higher tendencies of contraction and liquefaction properties. On the other hand, soil samples with a higher percentage of clay (ECS20 and ECS20) yielded the lowest PWP, with softening and dilative properties.

Keywords: porewater pressures; dynamic liquefaction; clayey sand; single degree of freedom; shaking table; east coast sand; amplification factors; earthquake-induced liquefaction

Citation: Kalatehjari, R.; Bolarinwa, A. Evaluation of Liquefaction Properties of East Coast Sand of New Zealand Mixed with Varied Kaolinite Contents Using the Dynamically Induced Porewater Pressure Characteristics. *Appl. Sci.* **2022**, *12*, 9115. https://doi.org/10.3390/app12189115

Academic Editor: Dongsheng Xu

Received: 28 July 2022
Accepted: 7 September 2022
Published: 10 September 2022

1. Introduction

It is a well-known fact to the geotechnical community that earthquake-induced soil liquefaction poses major damaging threats to the entire built environment, most notably in seismically active regions of the world (i.e., places located within the proximity of the ring of fire). Severe collateral damage was the consequence of earthquake-induced soil liquefaction in past earthquake events in New Zealand, such as the Kaikoura earthquake (Mw 7.8), which occurred on 14 November 2016; Canterbury earthquake sequence (CES) 2010–2011 (Mw 5.5 to 7.1), which happened between 4 September 2010 and 23 December 2011 [1]. An investigation of the area affected by CES [2] indicated seismically induced manifestations of liquefaction in Christchurch city of New Zealand as (i) lateral spreading and settlement-induced failure of bridges; (ii) failures of roads as a result of induced fissures and cracks on pavements; (iii) observed severe liquefaction ejecta (sand boils); (iv) massive collapse of lifelines, due to differential settlements and floatation; (v) impairment of port facilities, due to ground deformations and (vi) widespread differential settlements and tilting of

infrastructures, which summarily resulted in high collateral damage (huge economic loss), loss of lifeline (i.e., utilities), and in some cases, loss of lives. The economic losses resulted from the 2010–2011 CES were estimated 15 billion New Zealand Dollars [3,4].

The quest for sustainable, economic, environment-friendly, and effective means of mitigating earthquake-induced liquefaction necessitates the need to conduct more research/studies on composite or mixed soils, which are most likely encountered in fields. The common conventional liquefaction-mitigation methods work with the principles of densification, solidification, improvement of soil engineering properties, soil reinforcements, soil replacement, and drainage improvement-based techniques for water repellence [5,6]. Conventional and emerging soil liquefaction-mitigation methods are effective but are mostly associated with one or more limitations. Such limitations include poor cost feasibility associated with larger projects, negative environmental impacts/non-sustainable (due to introducing chemical agents), and disturbance to ancillary structures that are sensitive to deformation and vibrations, due to waves and disruptive installation effects [5,7–10]. More recently, [11] presented a review of the existing liquefaction mitigation methods and highlighted some limitations associated with them, indicating their effectiveness, applicability, duration time, durability, cost, and long-term observation. A tree diagram (infographic), broadly classifying the existing liquefaction mitigation methods, is summarized in Figure 1. The textbook soils referred to as clean sands and pure clays are well-researched, while in reality, in-situ soils are mainly composed of both cohesionless and cohesive particles. This necessitates the need to shift the research focus onto mixed soils for possible soil replacement alternatives/choices in small to medium-scale projects.

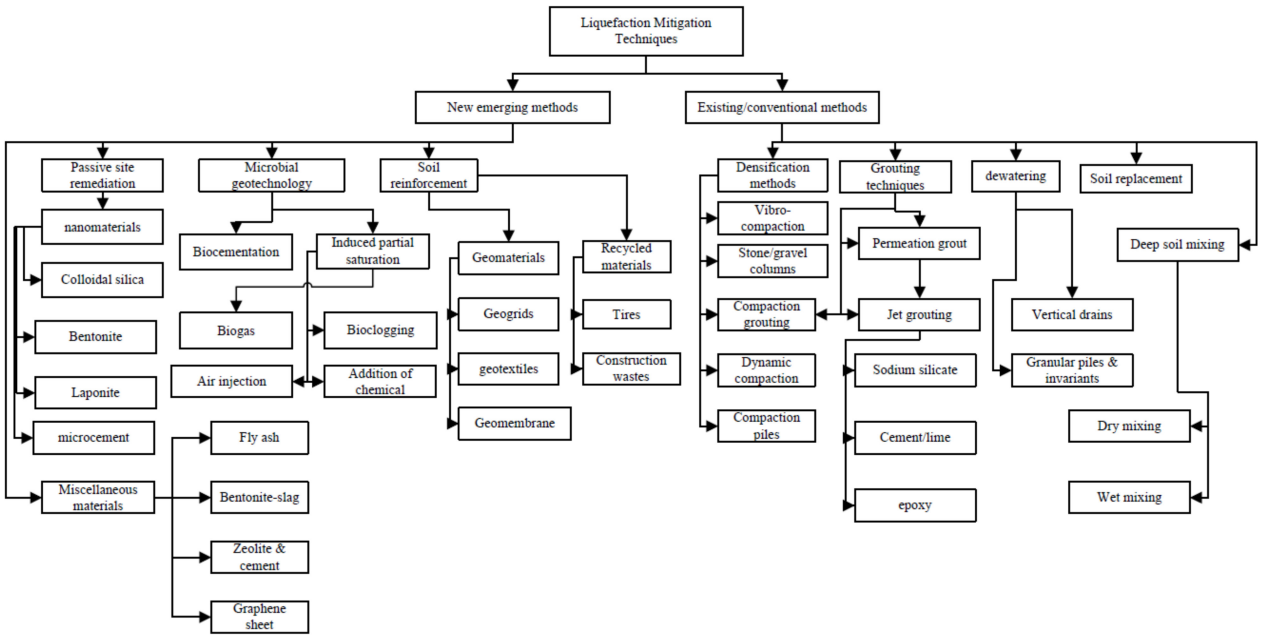

Figure 1. A summary of soil liquefaction mitigation techniques.

Varieties of physical model testing methods to mimic the effects of earthquakes on soils have evolved over the years and may broadly be classified into the following two groups: shaking table (ST) experiment (typically executed under the earth's gravitational field, i.e., 1 g) and geotechnical centrifuge experiment (performed under higher gravitational field). Although, the boundary effects and similitude/scaling laws on physical models executed in the laboratory are well-known challenges for adequate interpretation of model-prototype correlations. Consequently, previous researchers tend to study the dynamic characteristics of soils by utilizing large-scale models to make up for the boundary effects usually experienced in small-scale models. Nevertheless, it is still challenging to model in-situ soils with infinite lateral extents in a laboratory, with soil specimens confined in model containers of finite boundaries. Although, researchers have made several attempts

to mimic the infinite lateral extents with the application of the laminar shear box container types [2,3]. However, these soil container types cannot completely mitigate the restraints in lateral movements, as concluded based on a comprehensive review of the varieties of soil container types [4].

A review of the topic shows that large-scale physical model tests with the shaking table have associated advantages and limitations. Large-scale soil models' benefits may include experimenting with a substantial quantity of geomaterials to provide a near in-situ (i.e., field) response similar to the prototype soils. Possible minimal boundary effects may be attained, and the soil volume located around the central area of the soil model container is mainly considered an adequate representation of the free-field dynamics of the model soil. The control is possible for a large shaking table's input motion (i.e., 1-D, 2-D, 3-D, and multiples axis), and precise data measurement is probable [5]. On the other hand, limitations of large-sized, shaking table models may include the associated high cost of procurement and maintenance of actuators as the number of required actuators and payload increases [6]. In addition, large-size models often need outsized space to fit (or accommodate) the test setup, especially in small-spaced laboratories; the unavoidable long durations, laborious, and fatiguing requirements for sample preparations are notable associated limitations.

The scaling laws for the two-phase mechanics of soil-fluid physics are still not well-understood [7]. It is well-known, in principle, that the similitude laws in stress and strain cannot be satisfied in reduced-scale physical model ST experiments [6,8,9]. However, studies related to the evolution of excess porewater pressures (PWP) during earthquakes may conveniently be physically modeled with the advent of high-resolution transducers, coupled with a reduced-scale physical model setup. For instance, the above is helpful for studies that involve applications investigating earthquake-induced flow failures, landslides on slopes, possible liquefaction mitigation methods, retaining walls, pile–soil interactions, and seepage issues. Overall, modeling soil undrained behavior under shaking table conditions appears to be more realistic when compared with other laboratory testing methods, such as triaxial testing. This is because the stress conditions and measured deformations in soil samples tested under triaxial and other laboratory tests are greatly affected by boundary conditions. The applied loads do not mimic actual field situations, such as infinite lateral extents [10].

In the current study, a 600N rated capacity ST was designed and fabricated at the Auckland University of Technology (AUT) Geotechnical Laboratory to assess soil liquefaction-related mechanisms and the evolution of dynamic PWP, after considering the initially mentioned limitations of conventional large-scale shaking tables. The weights of all the prepared model soils were controlled with an electronic weighing scale to ensure that the model mass did not exceed the actuator's rated capacity (i.e., 600N). A parametric study was carried out to investigate the evolution of the dynamic excess PWP in east coast sand (ECS) and other artificially created clayey ECS by varying the kaolinite contents within the ECS fabrics with 5%, 10%, 15%, 20%, and 30% by weight kaolinite compositions. The idea herein is to implement a more economical methodology for initial assessment of geomaterials with more soil-water repellency properties, which may be applied in soil replacement schemes during earthworks/engineered fill construction works.

2. Materials and Methods

2.1. Description of the Designed and Constructed One-Dimensional 600N-Capacity Shaking Table

The ST assembly consists of an H-section sliding mechanism (Figure 2a,b), an actuator (MS500-Series Modal Shakers, Tenlee Electric Group, Wenzhou, China), an amplifier (Series LA-500, Tenlee Electric Group, Wenzhou, China), and a 25 mm thick plywood upper base (measuring 520 mm × 400 mm) screwed to the actuator and sliding mechanism with four M-8 bolts (Figure 2c,d). A 20 mm thick base plywood material measuring 1000 mm × 450 mm (i.e., length × breadth) houses the entire shaking table assembly and is connected to 4 nos of steel legs, with a 200 mm × 200 mm cross-section filled with concrete

to provide stability to the table as a reaction mass (Figure 3a). The amplifier powers the actuator, which moves the upper base plywood in a single degree of freedom (SDOF), simple harmonic motion. The ST assembly with the instrumented soil box (Figure 3b) operates according to the SDOF input ground motion theory. As per [11], Equation (1) is the governing physics for the motion vibration of a typical SDOF, shown schematically in Figure 4, based on Newton's 2nd law.

$$m\ddot{u} + c\dot{u} + ku = P(t) \quad (1)$$

where $P(t)$ is an externally applied dynamic load but here, $P(t) = 0$; m = mass of the soil model; $\ddot{u}$ = horizontal acceleration; $\dot{u}$ = horizontal displacement of the body; u = distance; k = spring of stiffness; c = viscous damping coefficient. Therefore, the sum of the inertia force, damping force, and spring force are equivalent to zero in Equation (1) for the equilibrium. The symbol dot notation signifies the required integral steps to achieve the symbolic variable.

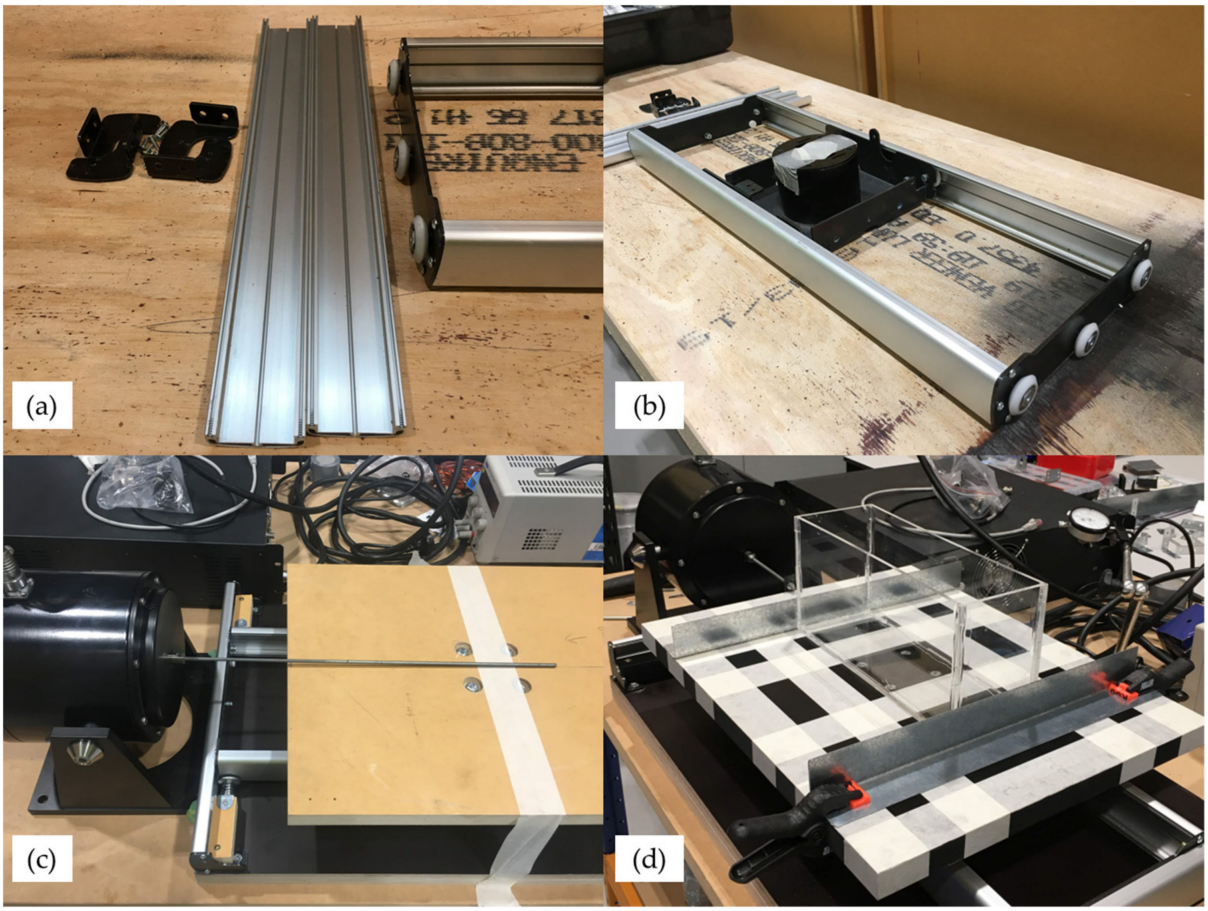

Figure 2. The sliding mechanism assembly for the shaking table. (**a**) Main parts of the sliding mechanism. (**b**) The sliding mechanism assembly. (**c**) The table and actuator assembly. (**d**) The adjustments and calibration of the shaking table.

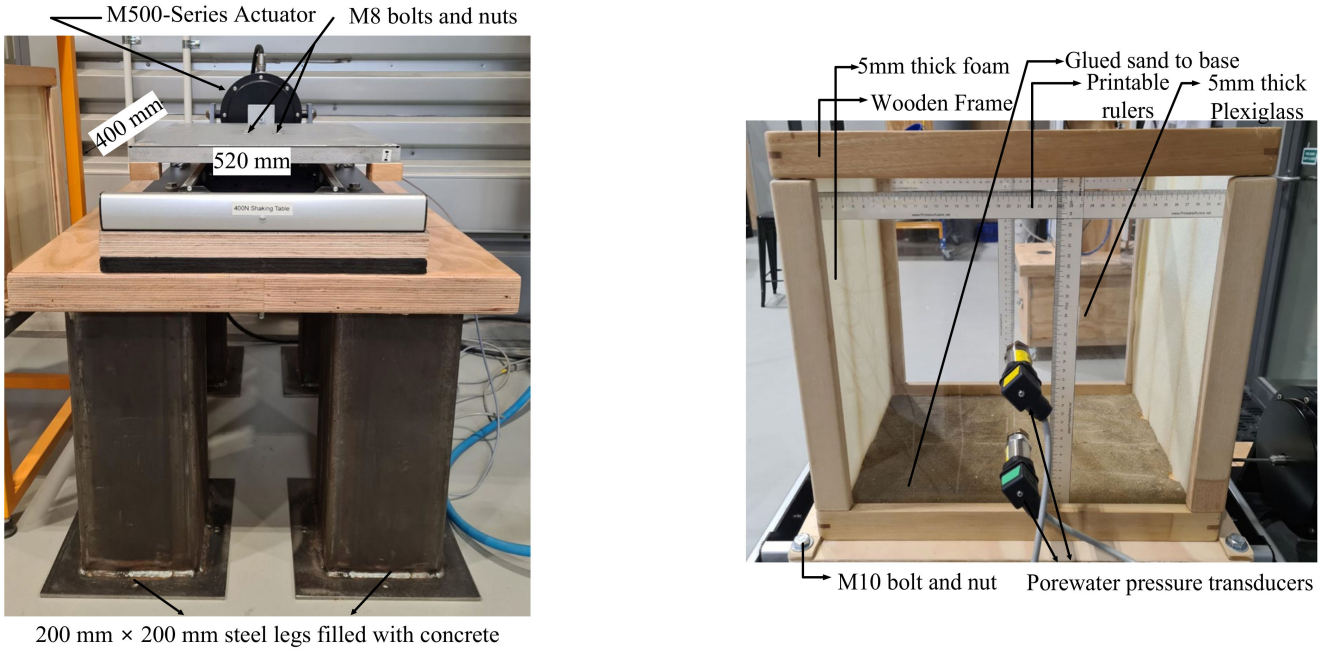

(**a**) (**b**)

Figure 3. The shaking table setup and main components. (**a**) The shaking table assembly. (**b**) The designed and fabricated soil rigid box/container.

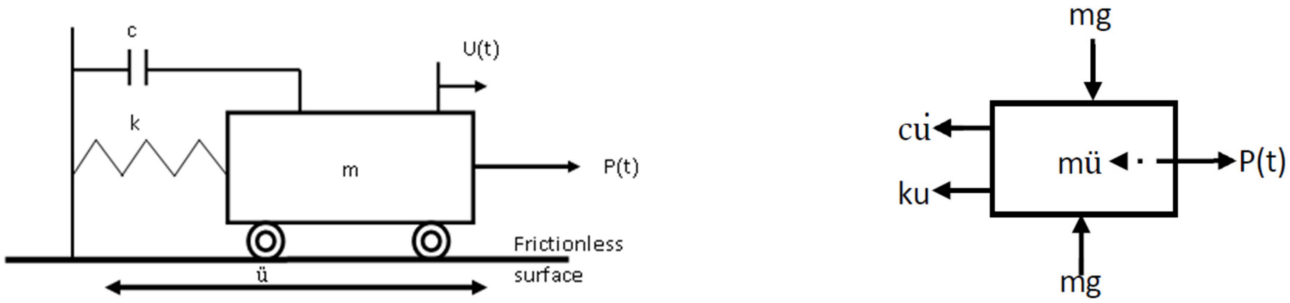

(**a**) (**b**)

Figure 4. Mechanics of typical SDOF motion for earthquake ground motion modeled on [11]. (**a**) The typical mass–spring–damper (MSD) model. (**b**) The free-body diagram (FBD) of the shaker setup.

The designed, constructed, and instrumented rigid soil box (SB), made of a 5 mm thick plexiglass material, has a total internal dimensional capacity of 395 mm × 295 mm × 400 mm (i.e., length × breadth × height). The SB is brazed around its external corners/edges, with timber frames to complement its strength and rigidity when subjected to high shaking intensities. Ref. [12] suggested that an absorbing material should be installed on the model rigid container's internal transient boundaries to minimize the effects of the artificial boundaries on the soil model. Following the above work, a foam material with a thickness of 5 mm was installed on the soil box internal transient boundaries. Dry sands were also glued to the box's base to aid the generation of upward shear stresses/waves in the specimen-soil model (refer to Figure 3b).

Printable rulers were glued to the inside of the container to accurately measure the container's internal size, soil sample heights, falling height during pluviation, and easy estimation of densities and water level. In addition, a data acquisition (DAQ) program was written in LabVIEW version 18.0.1 to develop an intuitive and interactive graphical user interface (GUI) for various inputs and outputs of the test setup.

2.2. Description of the Tested Soil Specimens

The tested primary sand specimen, east coast sand (ECS), is commercially mined from near the shore of Pakiri Beach, Mangawhai, north of Auckland, in the North Island of New Zealand. The sand is an alluvial product of the mechanical weathering of the Pakiri Group sandstone. The artificially created clayey invariants of the sand were derived by mixing the ECS with 0, 5, 10, 15, 20, and 30 percent by weight of kaolinite clay. The adopted naming nomenclature of the reconstituted model soil specimens are ECS00, ECS05, ECS10, ECS15, ECS20, and ECS30.

The scanning electron microscope (SEM) results obtained at the ×50 magnification scale indicated that the shape of ECS is sub-angular to angular, according to the visible geometric description (refer to Figure 5). The executed classification tests include the ECS's particle size distribution (PSD) and hydrometer tests for the kaolinite clay. The corresponding derived unified soil classification system (USCS) of ECS is a poorly graded sand (SP) material, the kaolinite is classified as a lean clay (CL), and other soil mixtures are mostly classified as clayey sands (SC), as shown in Table 1.

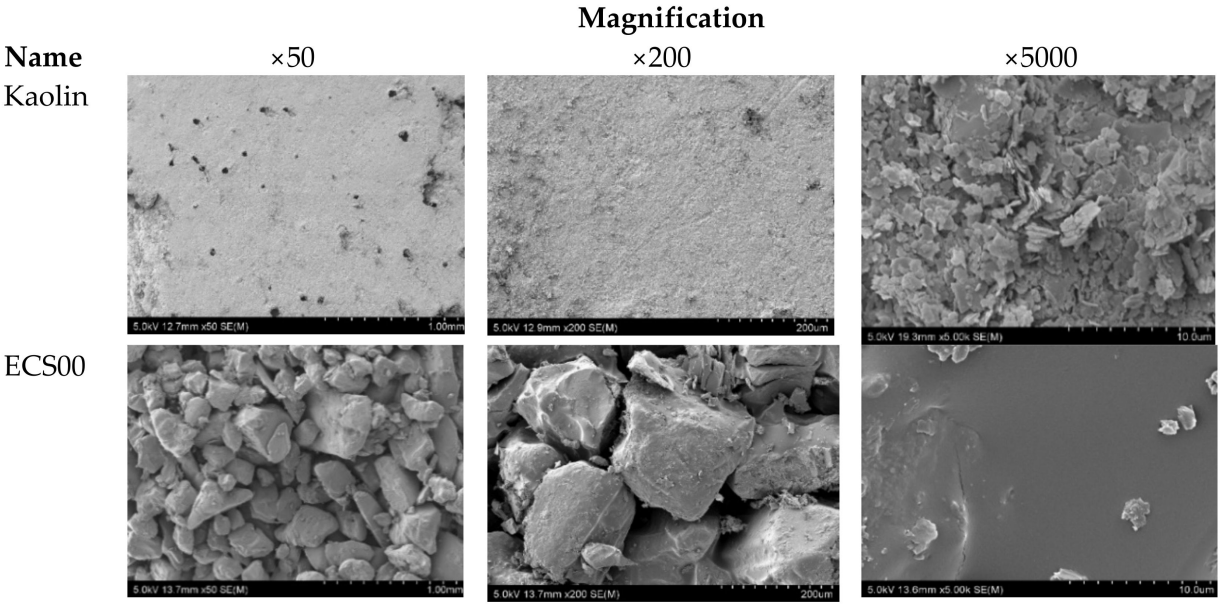

Figure 5. SEM micrographs of kaolinite and east coast sand (ECS00).

Table 1. The derived unified soil classification system (USCS) of all studied soil specimens.

Sample ID	C_u	C_c	*PI*	Fines (%)	Classification Based on ASTM D2487-17 [13]	USCS Description and Symbol
ECS00	1.63	0.96	NA	NA	$C_u < 6.0$ and $C_c < 1.0$	Poorly graded sand (SP)
ECS05	NA	NA	NA	5	$C_u < 6.0$ and $C_c < 1.0$	Poorly graded sand (SP)
ECS10	NA	NA	2	10	5–12% fines	Poorly graded sand with clay (SP-SC)
ECS15	NA	NA	5	15	>12% fines	Clayey sand (SC)
ECS20	NA	NA	7	20	>12% fines	Clayey sand (SC)
ECS30	NA	NA	9	30	>12% fines	Clayey sand (SC)
KK00	NA	NA	15	100	*PI* > 7 plots above the "A" line	Lean/inorganic clay (CL)

2.3. Soil Sample Preparation and Model Setup

The most tasking part of the model preparation procedures is shown in Figure 6. As per the preliminary sample preparations, the clean sand (ECS) and the industrial kaolinite were oven-dried between 50 and 70 °C for 24 h. Dry mixing by utilizing the mechanical mixer, as shown in Figure 6a, produced the mixed samples derived from both ECS and

sand-kaolinite sand matrix mixtures. For all the studied soil samples, dried specimens were pluviated into the soil container using a manual pluviator, as shown in Figure 6b. Pluviated samples were then saturated with de-aired water from the side of the model and left to equilibrate for a minimum time of 72 h [14]. The de-aired water with 72 h resting time was used to ensure saturation, since it is impractical to carry out a B-value check to confirm the degree of saturation for the soil specimen. The soil specimens were covered by plastic wrap during this time to prevent the evaporation and further aeration of the de-aired water.

(**a**) (**b**)

Figure 6. Sample preparations for shaking table experiment. (**a**) Dry mixing of east coast sand and kaolinite. (**b**) Dry pluviation of soil samples into the instrumented soil box.

The combined influence of effective confining stress and density/void ratios directly determines the liquefaction behavior of particulate materials, such as sand. Soil models were prepared with the configuration of low densities to simulate the in-situ evolution of dynamic excess PWP characteristics of liquefiable deposits in the laboratory. This approach was selected to make up for the effect of low confining stress and was similar to similar research found in the literature [15,16]. Most of the prototype model setup procedures followed the guidelines of the liquefaction experiments and analysis project (LEAP) [14,17] to ensure the replicability and repeatability of the sample preparation.

The utilized national instruments chassis is the model PXIe-1078 coupled with suitable VI data cards and other hardware, as schematically shown in Figure 7a; the plan and longitudinal view of the test instrumentation are shown in Figure 7b,c, respectively. The applied instrumentation includes accelerometers of model 4030-series, manufactured by TE Connectivity (TE.com/sensorsolutions accessed on 20 July 2022), and flush pressure sensors of SS402 series, manufactured by Sendo-Sensor (sendo-sensor.com accessed on 20 July 2022). An accelerometer installed on the shaking table base allowed us to measure/capture the input base motion of the acceleration-time histories. Another accelerometer was placed at approximately 200 mm depth at the near-surface level inside the soil models to study the amplification and attenuation characteristics of the tested soils. Two PWP transducers

were installed on the soil box at depths of about 100 mm and 200 mm to capture the PWP at the model's mid-depth and near-surface levels, respectively. All the sensors were connected and calibrated with the LabView DAQ system. All the soil models were shaken for about 15 s with a sine wave ground motion of constant frequency of 10 Hz and different amplitudes of 2, 3, and 4. The achieved testing peak ground acceleration (PGA) ranged between 0.1 g and 0.5 g.

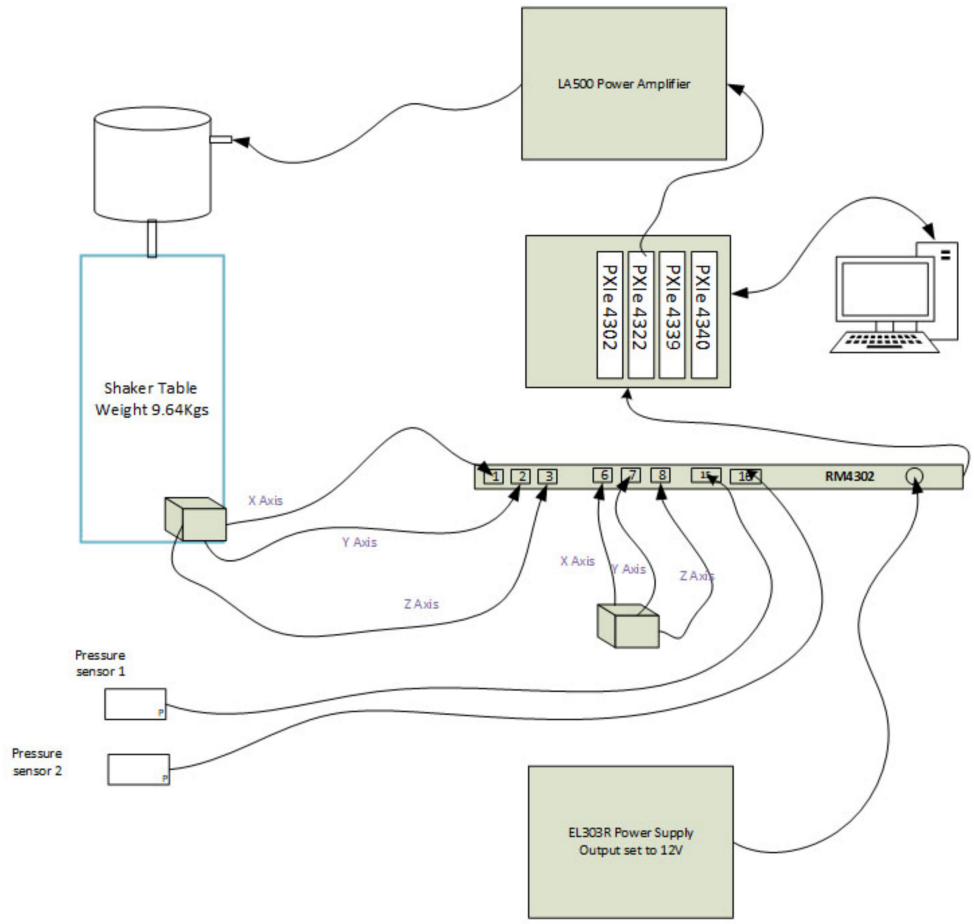

(**a**)

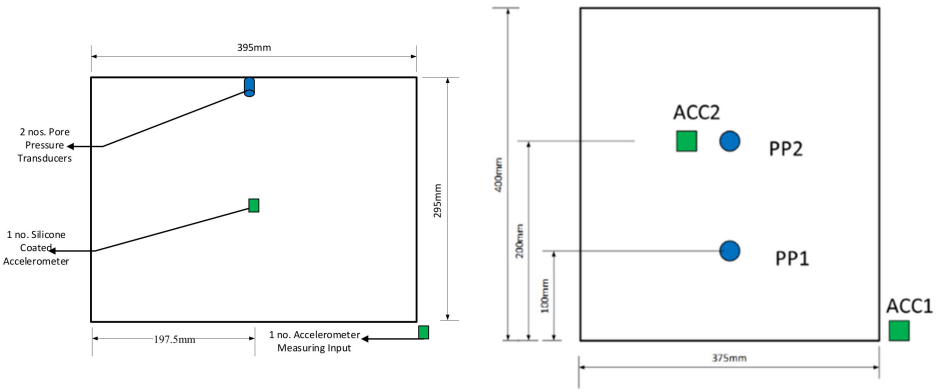

(**b**) (**c**)

Figure 7. Layouts of the test instrumentation. (**a**) Schematics of the hardware setup. (**b**) Plan view of test instrumentation. (**c**) Side view of test instrumentation.

3. Results

3.1. Soil Index Characteristics

The soil phase relationships were applied in the estimation of the basic soil index characteristics of all the studied samples, and they are summarized in Table 2. Under laboratory conditions, it is particularly challenging to create similar initial overburden effective stresses, as the soil models' depths are low compared to actual in-situ soils. Table 2 shows that the estimated submerged unit weights are approximately the same except for ECS30, with some deviations.

Table 2. Summary of experimental shaking table-physical model properties.

Sample/Properties	Moist Mass (kg)	Dry Mass (kg)	Moisture Content (%)	Specific Gravity (Gs)	Wet Unit Wt. (kN/m^3)	Estimated Void Ratio	Relative Density (%)
ECS00	51.79	40.00	29.48	2.60	19.82	0.600	60
ECS05	49.59	39.94	24.16	2.54	18.98	0.600	77
ECS10	49.48	40.00	23.70	2.61	19.38	0.600	72
ECS15	49.36	40.04	23.28	2.53	19.33	0.590	76
ECS20	49.46	39.46	25.34	2.59	19.37	0.650	68
ECS30	49.50	40.02	23.69	2.56	17.73	0.540	77

The specific gravity (G_s) values of all the soil samples were determined as per ASTM-D854-14 (2014) and applied to the relevant soil phase relationships to derive the estimated void ratios. The masses (dry and wet) were quantified with a two decimal precision weighing scale.

3.2. Dynamically Induced Porewater Pressure Characteristics

The observed excess PWP at the lower transducer (PP1) for the clean sand (i.e., ECS00) was the highest throughout the 3-stage shaking for all the studied soil specimens. Figures 8–10 show the results of the evolution of excess dynamic PWP at the lower pore pressure transducer during the three shaking cycles for all the studied soil samples. From the graph legends, PP1 is the name of the pressure transducer installed at the lower end of the SB, F10 signifies the shaking frequency at 10 Hz, and A2, A3, and A4 represent the amplitudes of 2, 3, and 4, respectively. The confirmation of liquefaction in Equation (2) was executed by computing the excess pore pressure ratio (r_u), obtained by the ratio of the excess pore pressures (Δu) to the total effective stresses (σ').

$$r_u = \frac{\Delta u}{\sigma'} \tag{2}$$

The liquefaction parameter (r_u) has been used by several researchers, e.g., [6]. The breakdown of its interpretation is as follows:

- When $r_u \geq 1$, it implies the occurrence of full liquefaction (FL);
- If $r_u = 0.25$ to 0.70, the likelihood of partial liquefaction (PL) is reported;
- If $r_u = 0$, a no liquefaction case is reported (NL).

The number of cycles required for either FL or PL reduces as the kaolinite content decreases correspondingly. Soil samples with more kaolinite (i.e., ECS20 and ECS30) did not liquefy but showed strain-softening behavior and dilative tendencies at higher shaking intensities.

The scaling laws, known as the similitude laws, are well-known key factors for consideration while interpreting the physical model results of particulate material, such as soil, in shaking table testing with a finite boundary domain. The key factors that determine similitude per liquefaction physical models have already been discussed in the literature. The relevant and typical applicable scaling laws in the current study adopted those provided by [18] and are summarized in Table 3.

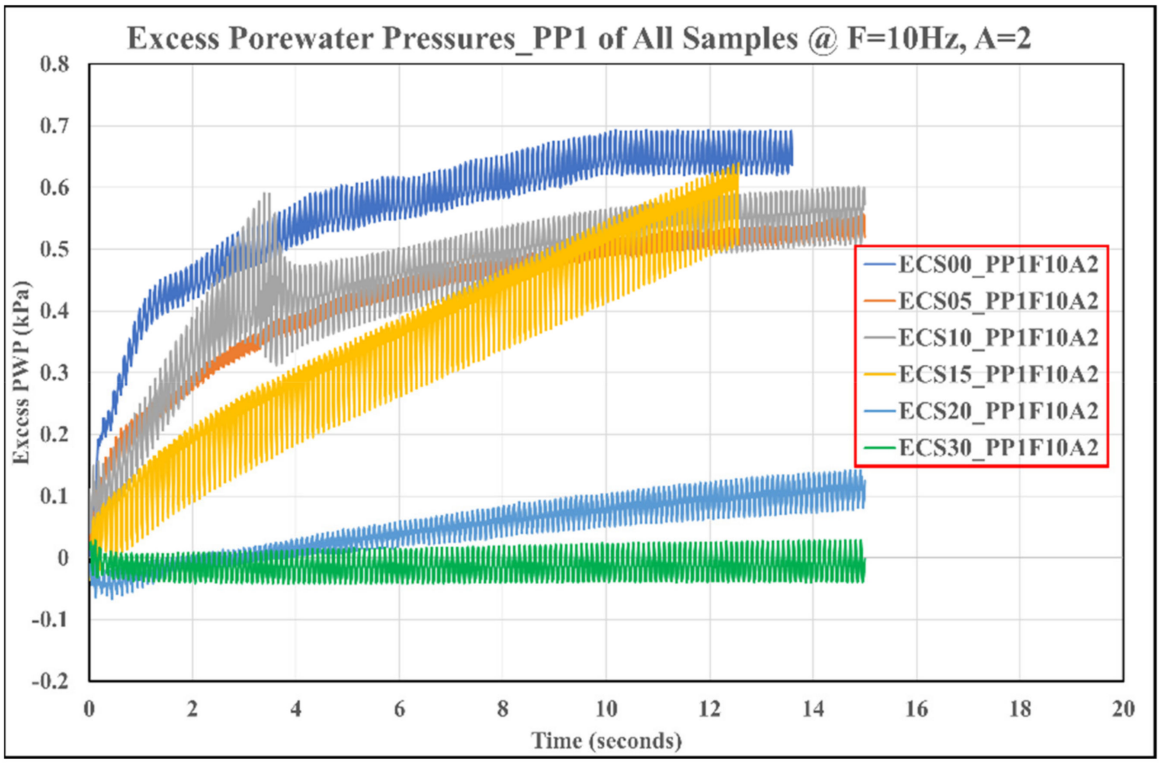

Figure 8. Excess PWP during the first shaking cycle.

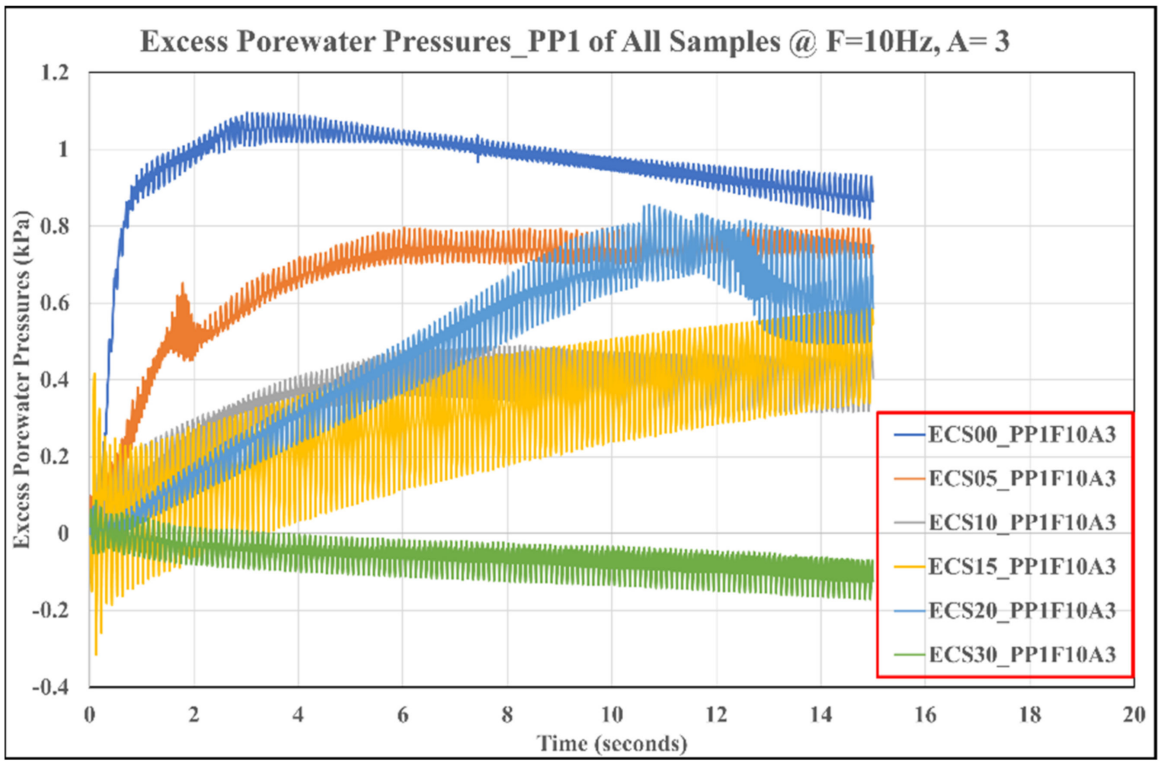

Figure 9. Excess PWP during the second shaking cycle.

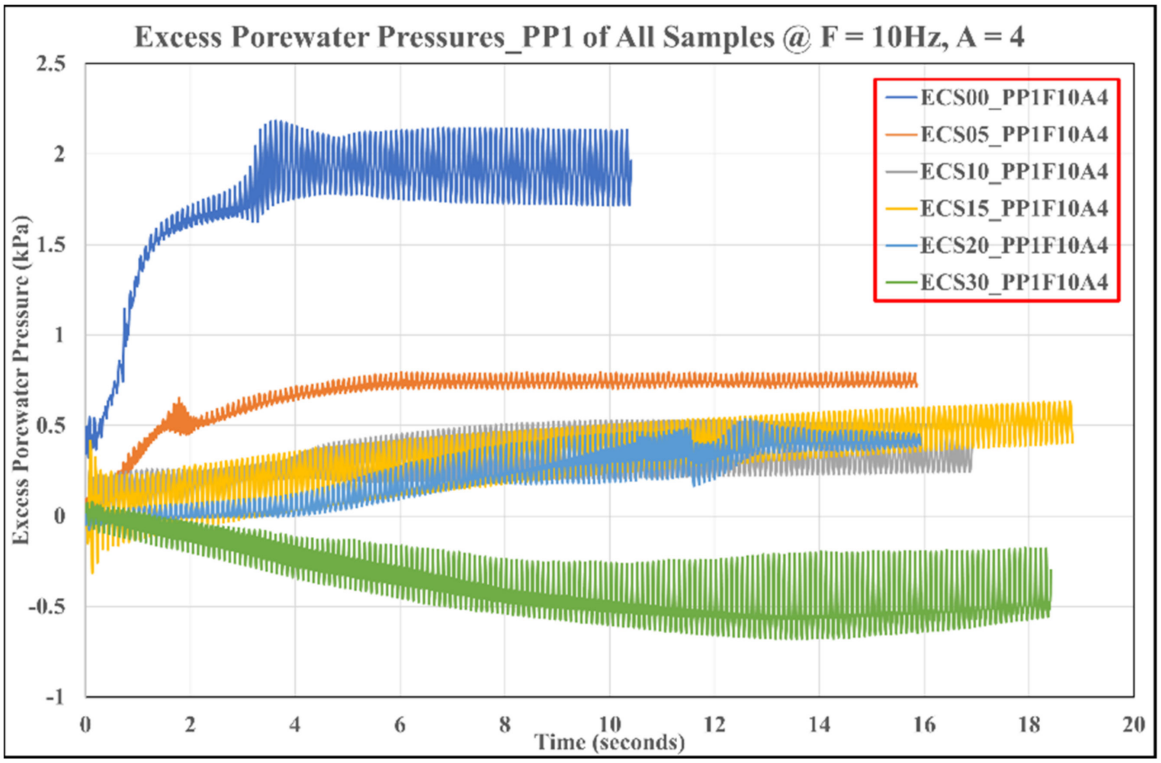

Figure 10. Excess PWP during the third shaking cycle.

Table 3. Summarized applicable similitude laws for shaking table as per [18].

Quantity Description	Symbol	Scaling Factors (Prototype/Model)
Length	l	λ
Saturated soil mass density	ρ_{sat}	1
Shear strain	γ	$\lambda^{0.5}$
Shaking time	t	$\lambda^{0.75}$
Total stress	σ	λ
Effective stress	σ'	λ
The bulk modulus of soil solid particles	K_s	$\lambda^{0.5}$
Pore water pressure	u	λ
Soil permeability	k	$\lambda^{0.75}$
Soil velocity	$\dot{u}$	$\lambda^{0.75}$
Soil acceleration	$\ddot{u}$	1
The relative displacement of pore water to soil skeleton	w	$\lambda^{1.5}$
Rate of flow of pore water	$\ddot{w}$	$\lambda^{0.75}$
Soil porosity	n	1
The bulk modulus of pore water	K_w	$\lambda^{0.5}$
Hydraulic gradient	i	1
Frequency	f	1
Shear modulus	G_{max}	$\lambda^{0.5}$

The fundamental physics used for deriving the scaling laws, as explained by [7], are typically governed by the fundamental laws of statics, which simulate the mass and force equilibrium of the soil structure, pore water, and the soil constitutive laws (i.e., the stress-strain characteristics). However, it is out of the scope of the current research to study the soils' deformation characteristics; instead, the main interest herein is the study of the evolution/generation of the soil-fluid/excess (PWP) mechanisms.

The soil-fluid similitude is complex, controversial, and poorly understood, as stated in the literature [7,18]. Overall, the significance of the similitude laws is their requirements

for interpreting the physical model results. Most importantly, the in-situ soil confining stresses are far greater than those produced in physical models. As found in [18], some soil parameters are significant parameters to scale with the similitude laws, including the ground thickness, soil density, small strain shear modulus, large-strain damping ratio, shaking circular frequency, acceleration, cyclic displacements, shear strain, and reference strain. In summary, the time scale in the model is reduced by the square root of the prototype time and the application of reduced soil densities (loose soils) in models for reasonable comparisons with prototype densities.

Figures 8–10 show that the dynamically generated excess PWP reduces as the clay contents within the fabrics of ECS increase, irrespective of the shaking intensities.

3.3. The Soil Dynamic Amplification Characteristics

The soil dynamic amplification factor (AF) is defined as the ratio of the horizontal peak ground acceleration (PGA) at the ground surface to the PGA from the bedrock or the earthquake acceleration ratio at which the earthquake acceleration would reach the ground surface [19]. One of the key parameters for earthquake-resistant designs is the PGA. This parameter helps to correctly predict when the magnitude of acceleration change from a bedrock would reach the ground surface. The derived AF values of the studied soil samples herein were computed as the ratio of the PGA from the ground accelerometer (AC2) to the PGA of the base input accelerometer (AC1). The observed patterns of computed AF were complex. The results were plotted on a three-dimensional statistical bar chart plot in Figure 11 to clearly illustrate the studied soils' amplification behavior.

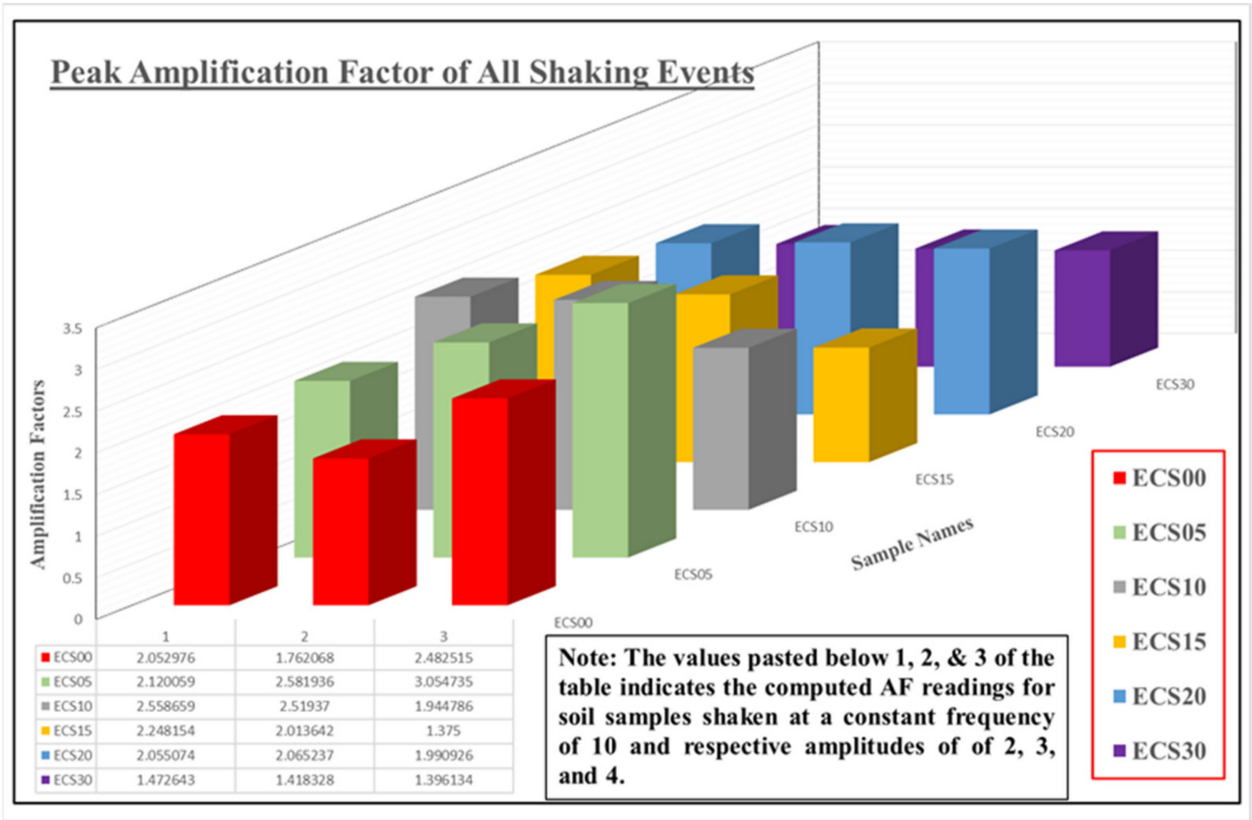

Figure 11. Statistical analyses of the amplification factors of all studied soil specimens.

4. Discussions

In practice, in-situ soil tests produce soil parameters with physical meanings for practical engineering applications. However, the soil samples used in this study were created in the laboratory. Thus, the results cannot be directly compared with in-situ soils,

without referencing the relative densities at which the tests were executed and applying the relevant similitude laws for the most suitable application interpretations. Moreover, a well-known issue is the problem of establishing correct model confining stresses relative to the high confining stresses inherent in prototype in-situ soils [18]. On this basis, model shaking tests are performed at low confining stresses (i.e., extremely loose deposits) to compensate for the effects of reduced geostatic stresses compared to in-situ soils. Therefore, the scaling or similarity laws, known as the similitude laws, are relevant to the logical interpretations of physical test results. As it is practically impossible to meet all the scaling laws requirements, most researchers only select a few key model parameters for scaling. The key elements for the investigation in the current study are itemized as follows:

(1) Investigating the dynamically generated excess porewater pressures (PWP) of the studied soil specimens, as a result of the varied clay (kaolinite) contents embedded in the fabrics of the ECS,
(2) Computing the amplification factors (AF) of all the studied soil samples,
(3) Observations and records of the seismically induced immediate settlements based on the sensitivity influences of the varied kaolinite contents in ECS,
(4) Studying the effects of recurring earthquakes on liquefaction extents by successively varying the intensities of base input motions.

The scenario in item 4 is mainly referred to as aftershocks, which are most common during actual earthquake occurrences in real-life situations. It is interesting to understand the response of the investigated soil samples under this condition.

As can be inferred from Figure 11, the soil sample with the highest amount of kaolinite exhibited the lowest AF, suggesting that the PGA would likely travel slower in soils containing clays. The granular structural arrangements of cohesionless materials, such as sand, with particle-to-particle contact would experience faster travel of the PGA emanating from bedrocks. Due to limited research funds and resources, other soil dynamic deformation properties were considered out of scope in the current study but are recommended for further studies. Surface settlement, measured with the printable rulers on the soil container, indicated that the immediate soil settlement was highest in the clean ECS sand and soil samples with more clay. This is because clean sands and clays are highly contractive; the highly contractive soil samples are ECS00, ECS20, and ECS30. A reduced immediate settlement was observable with moderate contents of kaolinite.

5. Conclusions

This paper presents the design, fabrication, and calibration of a modal shaking table for studying the dynamic characteristics of soils. The current study focused on the r_u coefficient method for evaluating soil liquefaction evolution by studying porewater pressure mechanisms. A parametric study of the dynamic excess porewater pressure generation characteristics and amplification factors of the remolded soil samples were conducted with a novel shaking table, and the results are summarized herein.

The clean east coast sand (ECS00) sample liquefied at full-scale throughout the three shaking events, while other samples with low clay (kaolinite) content (i.e., ECS05 and ECS10) exhibited either full or partial liquefaction during either the first, second or third shaking events. The samples with higher kaolinite content (i.e., ECS20 and 30) did not liquefy based on the observed r_u values.

The sand sample with no clay content (ECS00) exhibited the highest manifestation of liquefaction susceptibilities and other seismically induced failure-related mechanisms. Upon completion of the initial tests using the fabricated small shaking table, further analyses were carried out under the undrained monotonic triaxial compression tests for the clean ECS00 and ECS30 for advanced study of the behavior of these soils, as they showed the most extreme generated excess PWP characteristics.

The presented small shaking table device facilitated the parametric study of varieties of remolded soil samples in the laboratory. Observations from the study indicated and confirmed the comparative liquefaction characteristics of a wide range of samples with

varying clay (kaolinite) contents. Parametric studies with the application of large-scale, conventional shake tables are still relatively scarce in the literature. The scarcity of these studies is not far-fetched, as these tests could be overly costly, time-consuming, and laborious to prepare the required size of the physical soil models.

Author Contributions: Conceptualization, R.K. and A.B.; Data curation, A.B.; Formal analysis, A.B.; Funding acquisition, R.K.; Investigation, A.B.; Methodology, A.B.; Project administration, R.K.; Resources, R.K.; Software, R.K.; Supervision, R.K.; Validation, R.K. and A.B.; Visualization, R.K. and A.B.; Writing—original draft, A.B.; Writing—review and editing, R.K. and A.B. All authors have read and agreed to the published version of the manuscript.

Funding: This research was funded by the School of Future Environment, Auckland University of Technology through the project title "A novel small-scale, one-directional laboratory shaking table for quick assessment of seismic behaviour of soil" with funding number R12385.01.

Institutional Review Board Statement: Not applicable.

Informed Consent Statement: Not applicable.

Data Availability Statement: Data that support the reported results will be available by contacting the corresponding author upon reasonable request.

Acknowledgments: The authors would like to acknowledge the financial support from the School of Future Environment, Auckland University of Technology. Special thanks should also be given to the lab management and technicians at the School of Engineering, Computers, and Mathematical Sciences; without their technical support, this research could not have been completed.

Conflicts of Interest: The authors declare no conflict of interest.

References

1. Cubrinovski, M.; Henderson, D.; Bradley, B.A. *Liquefaction Impacts in Residential Areas in the 2010–2011 Christchurch Earthquakes*; UC Research Repository: Christchurch, New Zealand, 2012.
2. Bhattacharya, S.; Lombardi, D.; Dihoru, L.; Dietz, M.S.; Crewe, A.J.; Taylor, C.A. Model container design for soil-structure interaction studies. In *Role of Seismic Testing Facilities in Performance-Based Earthquake Engineering*; Springer: Berlin/Heidelberg, Germany, 2012; pp. 135–158.
3. Guoxing, C.; Su, C.; Xi, Z.; Xiuli, D.; Chengzhi, Q.; Zhihua, W. Shaking-table tests and numerical simulations on a subway structure in soft soil. *Soil Dyn. Earthq. Eng* **2015**, *76*, 13–28. [CrossRef]
4. Anastasopoulos, I.; Georgarakos, T.; Georgiannou, V.; Drosos, V.; Kourkoulis, R. Seismic performance of bar-mat reinforced-soil retaining wall: Shaking table testing versus numerical analysis with modified kinematic hardening constitutive model. *Soil Dyn. Earthq. Eng.* **2010**, *30*, 1089–1105. [CrossRef]
5. Dihoru, L.; Taylor, C.A.; Bhattacharya, S.; Wood, D.M.; Simonelli, A.; Moccia, F.; Mylonakis, G. Shaking table testing of free field response in layered granular deposits. In Proceedings of the 14th International Conference of Earthquake Engineering, Ohrid, North Macedonia, 30 August–3 September 2010.
6. Prasad, S.K.; Towhata, I.; Chandradhara, G.P.; Nanjundaswamy, P. Shaking table tests in earthquake geotechnical engineering. *Curr. Sci. India* **2004**, *87*, 1398–1404.
7. Iai, S. Similitude for shaking table tests on soil-structure-fluid model in 1g gravitational field. *Soils Found.* **1989**, *29*, 105–118. [CrossRef]
8. Mizuno, H.; Sugimoto, M.; Mori, T.; Iiba, M.; Hirade, T. Dynamic behaviour of pile foundation in liquefaction process—Shaking table tests utilising big shear box. In Proceedings of the 12th World Conference on Earthquake Engineering, Auckland, New Zealand, 30 January–4 February 2000.
9. Douglas, J. Earthquake ground motion estimation using strong-motion records: A review of equations for the estimation of peak ground acceleration and response spectral ordinates. *Earth-Sci. Rev.* **2003**, *61*, 43–104. [CrossRef]
10. Ueng, T.S.; Wang, M.H.; Chen, M.H.; Chen, C.H.; Peng, L.H. A large biaxial shear box for shaking table test on saturated sand. *Geotech. Test. J.* **2005**, *29*, 1–8.
11. Chopra, A.K. *Dynamics of Structures Theory and Applications to Earthquake Engineering*; Prentice Hall International: Eaglewood, NJ, USA, 1995.
12. Lombardi, D.; Bhattacharya, S.; Scarpa, F.; Bianchi, M. Dynamic response of a geotechnical rigid model container with absorbing boundaries. *Soil Dyn. Earthq. Eng* **2015**, *69*, 46–56. [CrossRef]
13. *ASTM D2487-17*; Standard Practice for Classification of Soils for Engineering Purposes (Unified Soil Classification System). ASTM International: West Conshohocken, PA, USA, 2017.

14. Kutter, B.L.; Carey, T.J.; Stone, N.; Bonab, M.H.; Manzari, M.T.; Zeghal, M.; Escoffier, S.; Haigh, S.K.; Madabhushi, G.S.P.; Hung, W.Y. LEAP-UCD-2017 V. 1.01 Model Specifications. In *Model Tests and Numerical Simulations of Liquefaction and Lateral Spreading*; Springer: Berlin/Heidelberg, Germany, 2020; pp. 3–29.
15. Motamed, R.; Sesov, V.; Towhata, I.; Anh, N.T. Experimental modeling of large pile groups in sloping ground subjected to liquefaction-induced lateral flow: 1-G shaking table tests. *Soils Found.* **2010**, *50*, 261–279. [CrossRef]
16. Varghese, R.M.; Latha, G.M. Shaking table tests to investigate the influence of various factors on the liquefaction resistance of sands. *Nat. Hazards* **2014**, *73*, 1337–1351. [CrossRef]
17. Kutter, B.L. *Model Tests and Numerical Simulations of Liquefaction and Lateral Spreading*; Springer Nature: Berlin/Heidelberg, Germany, 2019.
18. Towhata, I. *Geotechnical Earthquake Engineering*; Springer Verlag: Berlin/Heidelberg, Germany, 2008; Volume 1, p. 698.
19. Özdağ, Ö.C.; Gönenç, T.; Akgün, M. Dynamic amplification factor concept of soil layers: A case study in İzmir (Western Anatolia). *Arab. J. Geosci.* **2015**, *8.11*, 10093–10104. [CrossRef]